Journal of Applied Polymer Science

Structures and Properties of Easily Dyeable Copolyesters and Their Fibers Respectively Modified by Three Kinds of Diols

Changfei Fu, Lixia Gu
State Key Laboratory for Modification of Chemical Fibers and Polymer Materials, College of Material Science and Engineering, Donghua University, Shanghai 201620, People's Republic of China
Correspondence to: L. Gu (E-mail: gulx@dhu.edu.cn)

ABSTRACT: Three kinds of modified poly(ethylene terephthalate) copolyesters were synthesized, using sodium-5-sulfo-bis-(hydroxyethyl)-isophthalate as the third monomer, 1,3-propanediol (PDO), 2-methyl-1,3-propanediol (MPD), and 2,2-dimethyl-1,3-propanediol (neopentyl glycol or NPG) as the fourth monomer, respectively. The copolyester fibers were also prepared by melt spinning and drawing processes. The effect of PDO, MPD, and NPG on the synthesis and spinning process was investigated, and the structures and properties of both copolyesters and the produced fibers were characterized. The results exhibited that the structural difference of PDO, MPD, and NPG played an important role in the synthesis and spinning process, and significantly affected the structures and properties of both copolyesters and the produced fibers, which thereby resulted in the difference in terms of dyeability improvement of copolyester fibers. The dyeing at boiling temperature under normal pressure experiments of copolyester fibers in both disperse dyebath and cationic dyebath revealed that incorporation of the fourth monomer could improve the dyeability of copolyester fiber, and copolyester fiber containing MPD unit had better dyeability due to a looser, more accessible structure when compared with the fiber containing PDO or NPG unit. © 2012 Wiley Periodicals, Inc. J. Appl. Polym. Sci. 128: 3964–3973, 2013

KEYWORDS: copolyesters; fibers; properties and characterization; dyeability

Received 14 August 2012; accepted 21 September 2012; published online 16 October 2012
DOI: 10.1002/app.38633

INTRODUCTION

Poly(ethylene terephthalate) (PET) fiber has been widely used for textile materials because of its unique physical properties and wash-and-wear properties. However, its poor dyeability is one of major disadvantages due to lack of chemically active groups, high crystallinity, and tight amorphous structure, and its color by dyeing with disperse dyes is not bright and lively because of the nature of disperse dyes. Copolymerization of PET with ionic groups is an effective method to confer PET fiber cationic dyeability.[1] Cationic dyeable polyester (CDP) fiber containing 1–3 mol % sodium salt of 5-sulphoisophthalic acid (SIP) unit has shown an industrial success.[2] However, although there exist the sulfonate groups in CDP fiber which can exchange counterions with dye cations, the dyeing conditions of high temperature and high pressure are still required because of the relatively high crystallinity and compact amorphous structure.[3]

To improve cationic dyeability of CDP dyeing at boiling temperature under normal pressure, two main methods have been developed. One method is adding poly(ethylene glycol) (PEG) unit into CDP (known as easy cationic dyeable polyester, ECDP)[4,5]; however, ECDP has poor thermal stability because of the presence of thermally unstable ether bonds in PEG segments.[6] The other method is increasing SIP content in CDP (defined as high SIP content cationic dyeable polyester, HCDP)[7–9]; however, HCDP has the poor spinnablity because of the formation of ionic aggregates which act as thermo-reversible cross-links.[10,11]

One really impressive demonstration for improvement of CDP cationic dyeability is incorporating 2-methyl-1,3-propanediol (MPD) into CDP backbone, which is a novel approach to increase the accessiblity for dye molecule.[12,13] Three kinds of diols, i.e. 1,3-propanediol (PDO), MPD, and 2,2-dimethyl-1,3-propanediol (neopentyl glycol or NPG), have received much attention for modification of PET.[14–16] The related studies have revealed that addition of low content of PDO or MPD or NPG can reduce crystallinity and macromolecular regularity of PET; therefore, the improved dyeability of CDP can be expected by incorporating PDO or MPD or NPG into CDP backbone. However, there are no prior studies found adding PDO or NPG into CDP.

Because PDO, MPD, and NPG possess the same number of main chain carbon atoms but the different number of branched

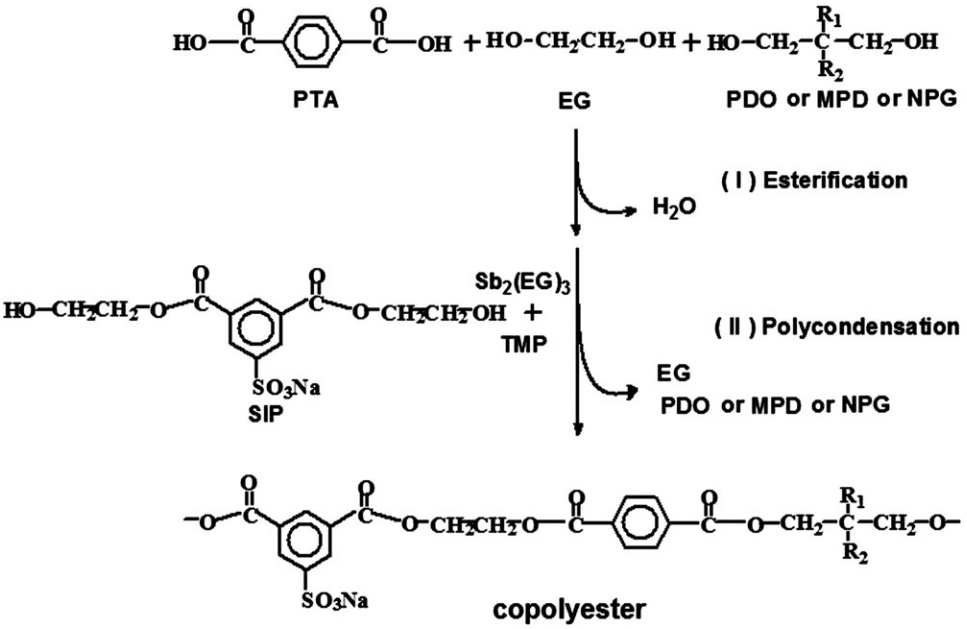

Figure 1. Synthetic scheme for preparing copolyesters. PDO: $R_1 = H$, $R_2 = H$; MPD: $R_1 = H$, $R_2 = CH_3$; NPG: $R_1 = CH_3$, $R_2 = CH_3$.

methyl groups, it is worth paying attention to the effect of PDO, MPD, and NPG on properties, especially, dyeability of copolyesters with the same proportion of co-units. This study reported our attempt to make an optimal selection on the fourth monomer among these three kinds of diols for cationic dyeable copolyester. Three kinds of modified PET copolyesters with the same feed molar ratio of comonomers were synthesized, using SIP as the third monomer, PDO, MPD, and NPG as the fourth monomer, respectively. The copolyester fibers with the same fineness were also prepared by melt spinning and drawing processes. For comparison, the fourth monomer-free copolyester with the same SIP content, i.e. CDP, was synthesized and CDP fiber with the same fineness was prepared. Our research focused on the effect of the structural difference of PDO, MPD, and NPG on the synthesis and spinning process, and the structures and properties, especially, dyeability of copolyesters.

EXPERIMENTAL

Materials

The comonomers used were: purified terephthalate acid (PTA; Sinopec Yizheng Chemical Fibre, China), ethylene glycol (EG; Sinopec Yangzi Petrochemical, China), 1,3-propanediol (PDO; Shell Guangzhou Petroleum, China), 2-methyl-1,3-propanediol (MPD; Lyondell Chemical, USA), 2,2-dimethyl-1,3-propanediol (neopentyl glycol or NPG; Jinan Shijitongda Chemical, China), and sodium-5-sulfo-bis-(hydroxyethyl)-isophthalate (SIP; Wujiang Wanda, China). Copolyesters were synthesized in the presence of ethylene glycol antimony ($Sb_2(EG)_3$) and trimethyl phosphate (TMP), which were used as received.

Synthesis of Copolyester

As shown in Figure 1, copolyesters were prepared using a PTA direct esterification and polycondensation route in a 20 -L reactor (Fourne Bonn, Germany). First, mixed diols (47.5 mol, the molar ratio of EG and the fourth monomer was 95:5) and PTA (30 mol) were put into a 20 -L reactor vessel. The reactor vessel was replaced by 0.1 MPa nitrogen at least three times to make sure that there was no residual oxygen inside the reactor before esterification. The stirrer was turned on at a stirring speed of 80 rpm. The temperature and pressure in the reactor were set at 210–250°C and 0.25 ± 0.01 MPa, respectively. The esterification was finished when about 60 mol of water as its by-product was discharged.

Next, the monomer SIP (0.45 mol), the catalyst $Sb_2(EG)_3$ (5.0 mmol), and the thermal stabilizer TMP (7.3 mmol) were added to the esterification product before polycondensation. The pressure in the reactor was gradually depressed to 100 Pa and the temperature was gradually heated up to 270°C within 45 min. During polycondensation, the stirring rate was adjusted from 80 to 40 rpm when the agitator torque boosted up to 65 Nm. The polycondensation was terminated when the agitator torque approached 100 Nm.

The prepared copolyesters containing PDO, MPD, and NPG were designated as PCDP, MCDP, and NCDP, respectively. The copolyester without adding the forth monomer, i.e. CDP, was also synthesized through the same procedures described above for comparison.

Preparation of Copolyester Fibers

Initially, the copolyesters were dried under vacuum at 110°C for 12 h. Next, the melt spinning experiments were performed by using ABE spinning equipment (Tokyo, Japan) with the take-up velocity of 800 m/min. All the copolyesters were spun to preoriented yarns with the same temperature settings; the temperatures of four zones in the screw were 282.0, 300.0, 295.0, and 295.0°C, respectively. Finally, the preoriented yarns were subjected to the posting-spinning drawing experiments by using TF100 parallel drawing machine (Suzhou, China) with the take-

Table I. Esterification Processing Parameters for Preparing Copolyesters

Sample code	Induction period[a] (min)	Total esterification time (min)	Total expellant water (mL)	Average expelled water	
				Rate (mL/min)	R^2 [b]
CDP	58	134	1050	13.8	0.994
PCDP	57	131	1050	14.2	0.991
MCDP	63	144	1050	13.0	0.983
NCDP	66	149	1050	12.7	0.985

[a]Defined as the time between system temperature up to 180°C and initial discharge water from fractionating column.
[b]Correlation coefficient in linear fitting.

up velocity of 370 m/min and the draw ratio of 3.7. The temperatures of the hot disc and hot plate during drawing were 80 and 165°C, respectively. All the copolyester fibers were controlled to the same fineness (100 denier/36 filament) for comparison.

Measurement and Characterization

Fourier transform infrared (FTIR) spectra were obtained using Nicolet 8700 IR spectrometer at room temperature from powder-pressed pellet samples in KBr. ^{1}H and ^{13}C NMR spectra were recorded on Bruker Avance 400 NMR spectrometer at 25.0°C operating at 400.1 and 100.6 MHz, respectively. About 50 mg copolyester was dissolved in 0.5 mL trifluoroacetic acid, and spectra were internally referenced to tetramethylsilane. The intrinsic viscosity (IV) of the copolyesters was measured at 25°C in an Ostwald viscometer using a solution of 130.0 mg copolyester in 25 mL phenol/carbon tetrachloride (3 : 2, w/w) as a mixing solvent. The diethylene glycol (DEG) content of the copolyesters was calculated from the relative integration areas of the protons resonances peaks of the methylene groups adjacent to ester alcoholic oxygen of DEG and all the diol units in ^{1}H NMR spectra. The carboxyl end group (CEG) content of the copolyesters was determined at room temperature using a solution of 300.0 mg copolyester in 25 mL phenol/carbon tetrachloride (3 : 3, v/v) as a mixing solvent titrated with a standard solution of KOH in methanol (20 mg/L), while three drops of a solution of 40 mg blue-bromophenol in 200 mL chloroform was added as an indicator. Color L and color b values of copolyesters were obtained using a GARDNER XL-20 colorimeter according to CIELAB scale. Differential scanning calorimetry (DSC) experiments of the copolyesters were performed under nitrogen atmosphere using a Perkin Elmer Diamond DSC instrument. Temperature and heat calibrations were carried out using pure samples of In and Sn. The copolyesters were melted at 280°C for 10 min until no residual crystals existed in the melt and then were quickly cooled to 40°C at a cooling rate of 50.0 K/min. The heating scan was started from 40 to 280°C at a heating rate of 10.0 K/min.

Wide-angle X-ray diffraction (WAXD) was used to determine the crystal structures and apparent crystallinity of copolyester fibers. WAXD experiments with a wavelength of 1.5418 Å were performed at beamlin 15 U, Shanghai Synchrotron Radiation Facility. The WAXD patterns were collected for 5 s using a Mar-345 CCD detector and then were integrated with FIT2D program. WAXD peaks were deconvoluted with the PeakFit v4 program by Jandel Scientific Software assuming Gaussian peak profiles. Mechanical properties of copolyester fibers were determined by using Shimadzu AGS-500ND universal material testing machine. Length between two holding jigs was 200 mm, and drop rate was 200 mm/min at room temperature. The measurements of dyeability of copolyester fibers were carried out using a laboratory scale Rapid Roaches dyeing machine. A total of 1.000 g copolyester fibers were placed in 2% owf Disperse Red HLE dyebath of a liquor ratio 50 : 1 and 2% owf Cationic Red X-GRL dyebath a liquor ratio 50 : 1, respectively. Dyeing time and dyebath temperature was 60 min and 100°C, respectively. The dye uptake value was determined by the absorbance of each dyebath solution before and after the dyeing via using a PerkinElmer Lambda 35 UV/visible scanning spectrophotometer. The dye uptake (D) was calculated by the follow equation,[17] where A_0 and A are the absorbance of the dyebath before and after dyeing, respectively.

$$D(\%) = \frac{A_0 - A}{A_0} \times 100\% \quad (1)$$

RESULTS AND DISCUSSION

Esterification and Polycondensation

Esterification processing parameters for preparing CDP, PCDP, MCDP, and NCDP copolyesters were given in Table I. During esterification, the amount of water discharged from the fractionating column was basically linear to esterification time as all the relative coefficients in linear fitting above 0.98. Because the average expelled water rate (the slope of linear fit) corresponded to the esterification rate,[14] the finding in terms of the expelled water rates showed that the addition of PDO accelerated esterification rate, whereas the addition of MPD and NPG successively decelerated esterification rate, and this conclusion was also supported by the data of esterification induction period and total esterification time in Table I. This could be explained from the electric effect and steric hindrance effect. The electronegativity of oxygen atom in PDO, MPD, and NPG was successively enhanced when compared with EG because of the donating electrons capability of both methylene and methyl groups, which benefited nucleophilic substitution during esterification between PTA and fatty diols.[18] In the case of PDO, the influence of the strengthened electronegativity of oxygen atom on the esterification rate was similar to Wei's study.[14] However, the oxygen atoms in MPD and NPG were more electronegative than that in PDO, but the esterification rate in the presence of MPD

Table II. Polycondensation Processing Parameters for Preparing Copolyesters

Sample code	Polycondensation temperature (°C)	Pressure (Pa)	Induction period[a] (min)	Total polycondensation time (min)	End agitator torque (Nm)
CDP	270	<100	10	125	100
PCDP	270	<100	15	132	100
MCDP	270	<100	20	137	100
NCDP	270	<100	30	143	100

[a]Defined as the time between system pressure up to 100 Pa and agitator torque starting to increase.

and NPG decreased in succession. This result could mainly attribute to the steric hindrance effect of branched methyl groups, which played negative effect on the nucleophilic attack the carbon atom of carbonylic group in coordination of two PTA; therefore in the presence of MPD and NPG, the steric hindrance effect probably became the dominant factor to affect the esterification rate.

As shown in Table II, PDO, MPD, and NPG in succession extended the induction period of polycondensation, and also successively lengthened the total polycondensation time, implying that polycondensation became more difficult in the order of CDP, PCDP, MCDP, and NCDP as the dynamic viscosity of the polymer melt increased with increasing molecular weight. On one hand, the steric hindrance effect of branched methyl groups was considered as a factor to hinder the formation and breaking of a chelate ring on antimony which was regarded as the rate-determining step during polycondensation.[19] On the other hand, the boiling points of PDO, MPD, and NPG are 214.4, 214, and 210°C, respectively, which are higher than that of EG (197.3°C), resulting in lower volatility in comparison with that of EG. Therefore, it got difficult for PDO, MPD, and NPG to diffuse in the melt when the melt viscosity reached a certain value, which led to the extended polymerization time.

Figure 2 showed the change of stirring torque versus polycondensation time. In each case, the stirring rate was 80 rpm before turning point but 40 rpm after turning point. It could be seen that in the late period of polycondensation, agitator torque increased significantly for preparing CDP and rose relatively steadily in the cases of PCDP, MCDP, and NCDP. For CDP, the phenomenon of the dynamic viscosity remarkably increasing could be the result of ionic aggregate of the sulfonate groups with an increasing SIP content in macromolecule,[10,11] which was also observed by other researcher.[20] The relatively linear growing of the stirring torque during the late polycondensation of PCDP, MCDP, and NCDP indicated that PDO, MPD, and NPG seemed to reduce ionic aggregate effect of sulfonate groups. This was probably due to that the relatively long main chain and(or) relatively bulky branched methyl groups of the fourth monomer increased the distance of SIP units in macromolecule chain.

Structure and Composition of Copolyesters

The FTIR patterns of the copolyesters in Figure 3 showed that CDP, PCDP, MCDP, and NCDP shared similar spectra with the strong characteristic absorption bands of polyester at 1722–1715 cm^{-1}(C=O stretching vibrations), 1263–1248 cm^{-1}(C(O)—O stretching vibrations), 1100–1097 cm^{-1} (C—O—C stretching vibrations), and 727–724 cm^{-1}(C—H in the benzene ring out-of-plane bending vibrations). The absorption bands of all the copolyesters at 1175 cm^{-1} and 624 cm^{-1}, assigned to the S=O and C—S stretching vibrations, respectively, indicated that SIP unit had been successfully polymerized into each copolyester. The strengthened intensity of the CH_2 wagging vibration

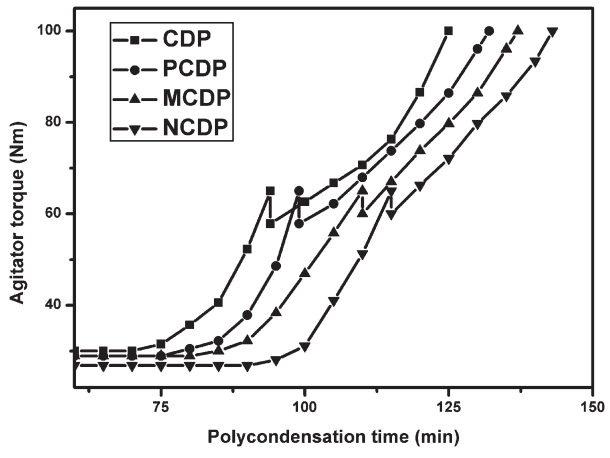

Figure 2. Agitator torque versus polycondensation time for preparing copolyesters.

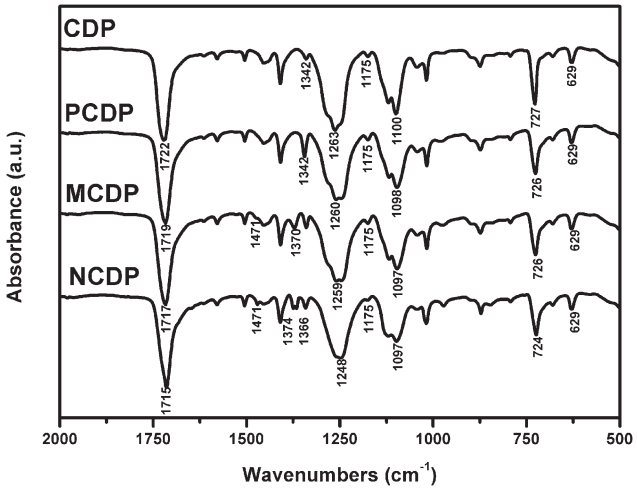

Figure 3. FTIR spectra of copolyesters.

Applied Polymer SCIENCE

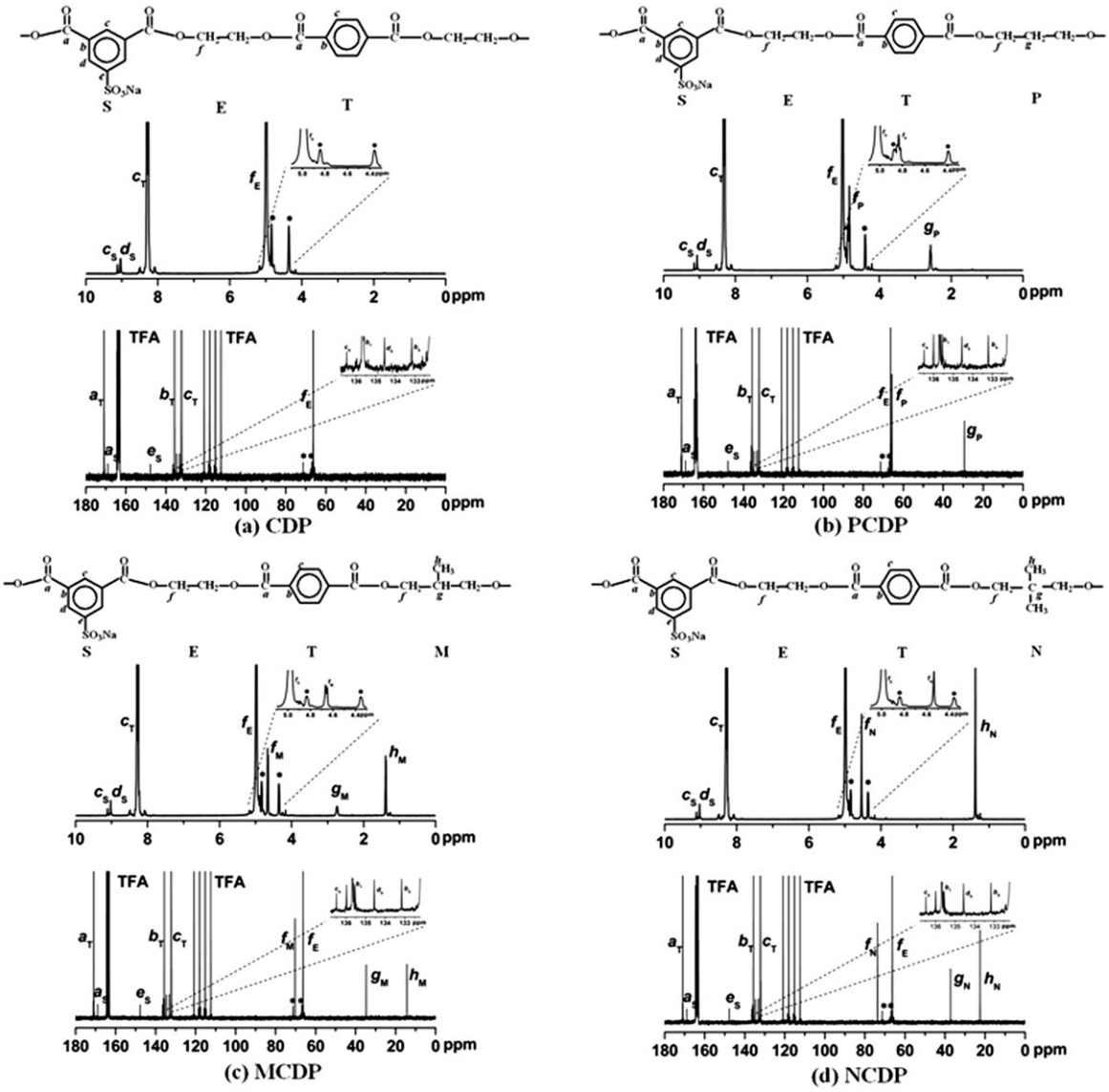

Figure 4. ^{1}H NMR (upper) and ^{13}C NMR (lower) spectra of copolyesters. The asterisk in ^{1}H NMR and ^{13}C NMR denotes DEG content. TFA in ^{13}C NMR represents deuterated trifluoroacetic acid.

absorption at 1342 cm^{-1} in the FTIR spectrum of PCDP, the C—H asymmetrical and symmetrical deformation vibration in the methyl group at 1471 and 1370 cm^{-1} in the FTIR spectrum of MCDP, the C—H symmetrical deformation vibration absorption band splitting into two new bands at 1374 and 1366 cm^{-1} because of the coupling effect of the two methyl groups connected to the same carbon atom in the FTIR spectrum of NCDP; these results suggested that PDO, MPD, and NPG units had been attached to PCDP, MCDP, and NCDP maromolecular chains, respectively.

Further characterization for the chemical structures of the copolyesters was obtained by NMR spectroscopy. ^{1}H NMR and ^{13}C NMR spectra of the copolyesters were shown in Figure 4, together with the chemical shift assignments. ^{1}H NMR and ^{13}C NMR spectra revealed clear differences in the chemical shifts of signals that arose from PTA, EG, SIP, PDO, MPD, and NPG units (abbreviated as T, E, S, P, M, and N in Figure 4, respectively) in macromolecules, as well as additional small peaks due to the presence of DEG unit (marked as asterisk in Figure 4). For all the copolyesters, both ^{1}H NMR and ^{13}C NMR spectra were found consistent with the anticipated structures. The inset figures of ^{1}H NMR spectrum showed that the hydrogens (f_P, f_M, and f_N protons) of methylene groups adjacent to ester alcoholic oxygen of PDO, MPD, and NPG units had three signals, two signals, and one signal, respectively. This was the result of spin–spin coupling effect of the adjacent hydrogens according to the n+1 rule.[21] The inset figures of ^{13}C-NMR spectrum showed that the aromatic quaternary carbons (b_T) of PTA unit in PCDP, MCDP, and NCDP split into one major peak and two small peaks of nearly equal intensity. Because the aromatic quaternary carbon was sensitive to neighboring units,[22] this could be attributed to the different sequence of EG unit and the fourth unit (PDO or MPD or NPG) centered at PTA unit.

Table III. Feed Molar Ratio and Composition of Copolyesters

	Feed molar ratio		Relative amounts from ^{1}H-NMR		Relative amounts from ^{13}H-NMR	
Sample code	SIP/PTA	Fourth monomer/EG	SIP/PTA	Fourth monomer/EG	SIP/PTA	Fourth monomer/EG
CDP	1.5/98.5	/	1.49/98.51	/	1.47/98.53	/
PCDP	1.5/98.5	5.0/95.0	1.47/98.53	6.10/93.90	1.45/98.55	6.12/93.88
MCDP	1.5/98.5	5.0/95.0	1.46/98.54	6.25/93.75	1.43/98.57	6.35/93.65
NCDP	1.5/98.5	5.0/95.0	1.43/98.57	6.16/93.84	1.43/98.57	6.26/93.74

The composition of copolyesters was determined from the relative integration areas of different resonances peaks in ^{1}H NMR and ^{13}C NMR spectra, respectively. The relative amounts of SIP/PTA and the fourth unit/EG in copolyesters could be calculated using the following equations:

$$\frac{\text{SIP}}{\text{PTA}} = \frac{(b_S + c_S)/3}{c_T/4} \quad (2)$$

$$\frac{\text{PDO}}{\text{EG}} = \frac{f_P}{f_E} \text{ (in the case of PCDP)} \quad (3)$$

$$\frac{\text{MPD}}{\text{EG}} = \frac{f_M}{f_E} \text{ (in the case of MCDP)} \quad (4)$$

$$\frac{\text{NPG}}{\text{EG}} = \frac{f_N}{f_E} \text{ (in the case of NCDP)} \quad (5)$$

The results were given in Table III, as well as the feed molar ratios. It could be seen that the values calculated from ^{1}H NMR were in good agreement with those calculated by ^{13}C NMR. Although the agreement found between copolyester composition and feed might be, overall, acceptable, the SIP unit content was slightly less than the feed molar ratio, whereas the fourth unit content was slightly more than the feed molar ratio. Similar to the other researches on the polycondensation of copolyesters containing isophthalate unit,[23–25] the slightly low SIP unit content in the prepared copolyester might be explained by the occurrence of side reaction cyclic dimerization of SIP during polycondensation. The fourth monomer possessed higher boiling point and lower volatility than EG, as mentioned earlier, thereby it was more difficult to extract during polycondensation, resulting in the slight richness of the fourth unit content in the prepared copolyester. More importantly, the very little divergence of the SIP unit contents and the fourth unit contents might be considered within experimental error. In other words, for all the copolyesters the SIP contents were nearly identical, and PCDP, MCDP, and NCDP possessed almost the same contents of PDO, MPD, and NPG units, respectively.

The other relevant characteristics including the IV values, DEG contents, CEG contents, and color of copolyesters were listed in Table IV. Although the terminational stirring torque reached the same value (100 Nm) in each polycondensation reaction system, the IV values of the copolyesters utilizing the fourth monomers was slightly higher than that of CDP. Because the fourth unit segment was more flexible than EG, the higher molecular weight was needed when the copolyester melt reached the same dynamic viscosity. As the chain mobility was hindered by branched methyl groups, the IV values of PCDP, MCDP, and NCDP decreased in succession. However, the difference of the IV values for the copolyesters was very little (0.500–0.518 dL/g); therefore, it was not considered as an important factor affecting the following spinning process.

It was well known that producing DEG unit was one of the characteristic side reactions during esterification of polyester or copolyester.[26] The DEG content slightly decreased in the order of CDP, PCDP, MCDP, and NCDP, probably relating to the dilution of EG concentration by the relatively bulky fourth monomer. Lower DEG content benefited the thermal stability of copolyester because of the presence of thermally unstable ether bonds, but disadvantaged to the dyeability of the copolyester fibers due to the flexibility of DEG segments.[27]

CEG, formed from thermal decomposition of copolyester during polycondensation, was also an important parameter to predict the stability of copolyesters due to the influence of CEG on thermal and hydrolytic degradation of copolyesters.[26] The CEG content decreased in the order of CDP, PCDP, MCDP, and NCDP, suggesting the improvement of the thermal stability.

The color of copolyesters was important in view of economical and practical point. According to the CIELAB scale, greater *L* value was desirable, meaning higher degree of whiteness, and greater *b* value was undesirable, signifying higher degree of yellowness. As shown in Table IV, *L* values, usually associated with the reduction of the Sb^{3+} catalyst to finely divided metallic antimony, showed a very little difference, indicating that the effect of the fourth monomer on *L* value of the prepared copolyester was not important. However, *b* values, usually associated with yellow byproducts of degradation of macromolecules, increased in the order of CDP, PCDP, MCDP, and NCDP, suggesting that

Table IV. Intrinsic Viscosity, DEG Content, CEG Content, and Color of Copolyesters

Sample code	IV (dL/g)	DEG (wt %)	CEG (mol/t)	Color	
				L-value	*b*-value
CDP	0.500	3.88	17.43	61.9	2.93
PCDP	0.518	3.42	15.21	62.2	3.36
MCDP	0.512	3.35	13.74	60.9	3.84
NCDP	0.505	3.22	13.36	60.3	6.17

Applied Polymer SCIENCE

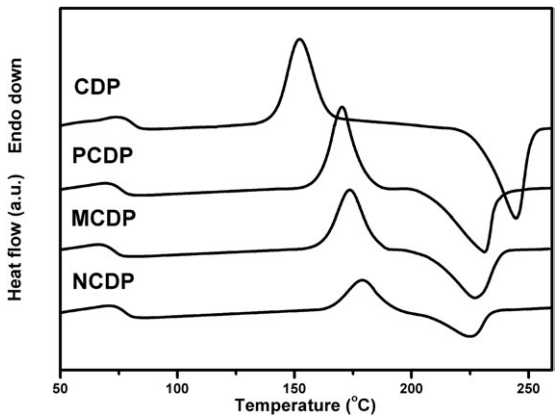

Figure 5. DSC thermograms of copolyesters after clearing up heat history.

the extended polymerization time deteriorated the color of copolyester. The colorimetric data were consistent with visual examination, and NCDP chips possessed the deepest yellow appearance when compared with the other copolyesters.

Phase Transition Behavior of Copolyesters

Figure 5 showed DSC thermograms of the copolyesters measured by heating with a rate of 10.0 K/min after clearing up their heat history. For each copolyester, apart from the glass transition (T_g), DSC curve revealed the exothermic transition peak due to cold crystallization above the baseline, and endothermal peak corresponding to the melting transition of crystals below the baseline. The results estimated from the DSC thermograms in Figure 5 were summarized in Table V.

In each case, a single T_g rather than two or more was observed, indicating that the distribution of the co-units in the prepared copolyester was essentially random. T_g moved to a lower temperature in the order of CDP, PCDP, and MCDP, implying that the fourth unit enhanced the chain flexibility and the free volume, and therefore, less energy was required for chain segment motion in amorphous region. However, T_g of NCDP was higher than that of both PCDP and MCDP; this might be the result of the steric hindrance effect of the branched methyl groups on chain segment motion.

From Figure 5 and Table V, it was evident that the cold crystallization temperature (T_{cc}) gradually increased and the cold crystallization enthalpy (ΔH_{cc}) successively decreased in the order of CDP, PCDP, MCDP, and NCDP, suggesting that more thermal energy was required for the molecular rearrangement in the process of nucleation and crystal growth. This decline of the crystallization ability resulted from the successive enhancement of the chain irregularity by introducing PDO, MPD, and NPG into the maromolecular chain.

The melting temperature (T_m) and the melting enthalpy (ΔH_m) were found to decrease as shown in Figure 5 and Table V in the order of CDP, PCDP, MCDP, and NCDP, accompanying with the gradually widening melting peak. First, the fourth unit in copolyester might shorten the length of crystallizable homopolymer's segment, and thereby reduced their crystallinity and crystal size. Next, the fourth unit might destroy the regularity of

Table V. Thermal Properties of Copolyesters in DSC Heating Scan

Sample code	T_g (°C)	T_{cc} (°C)	ΔH_{cc} (J/g)	T_m (°C)	ΔH_m (J/g)
CDP	79.1	152.3	28.9	244.5	−36.7
PCDP	74.2	170.8	25.3	231.7	−28.4
MCDP	71.2	173.8	22.2	226.8	−23.1
NCDP	75.8	179.4	11.8	224.9	−12.9

macromolecular chain which led to further reducing their T_m value. Finally, the branched methyl groups hindered the sequential arrangement of macromolecular chain, resulting in less perfect crystals. Therefore, PDO, MPD, and NPG successively played the more and more negative role in terms of crystallinity,

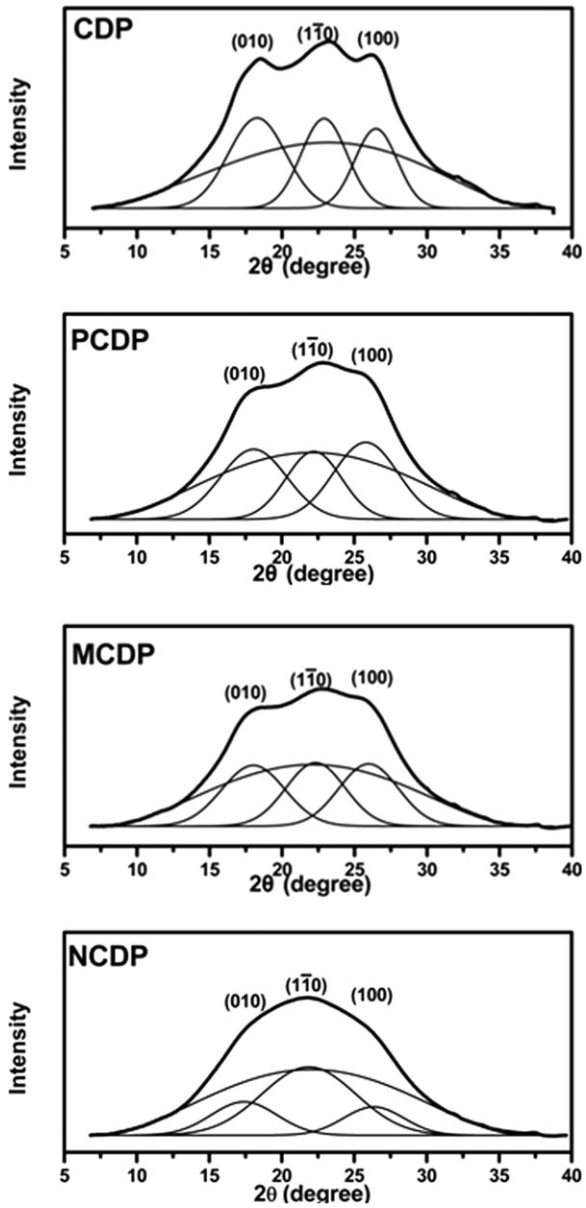

Figure 6. WAXD diffractograms for copolyester fibers.

Table VI. Crystallinity, Crystal Size, and Interplanar Distance of Copolyester Fibers

Sample code	Crystallinity (%)	Crystal size (Å)			Interplanar distance (Å)		
		(010)	(1$\bar{1}$0)	(100)	(010)	(1$\bar{1}$0)	(100)
CDP	48.4	24.78	31.32	34.18	4.85	3.88	3.37
PCDP	46.6	21.54	25.83	22.51	4.91	3.98	3.38
MCDP	44.1	20.55	22.06	22.06	4.92	4.00	3.43
NCDP	40.5	19.66	21.78	13.94	5.10	4.06	3.45

crystal size, and crystal perfection in the process of crystal formation.

Spinnability of Copolyesters

It was well known that the spinnability of copolyesters was affected by the structure and properties of copolyesters. In this study, for comparing the properties of the various copolyester fibers, the spinning and drawing process parameters, including take-up velocity, spinning temperature, draw ratio, and drawing temperature, were set up to the same for all the copolyesters. During spinning and drawing of CDP, PCDP, and MCDP, the pressure of the extruder screw remained constant and the winding process of both spinning and drawing maintained stable, showing excellent spinnablility and drawability. However, NCDP fiber was hardly wound onto the bobbin at the beginning of spinning. Fortunately, utilizing the approach of gradually increasing take-up velocity from 500 to 800 m/min, the final NCDP fiber was prepared with the same spinning and drawing conditions as the CDP, PCDP, and MCDP fibers. The 36 multifilament yarn finenesses of the prepared CDP, PCDP, MCDP, and NCDP fibers were 109.8, 109.4, 109.5, and 110.3 dtex, respectively, quite approaching to the expected fineness of 100 denier/36 filament.

Crystal Structure of Copolyester Fibers

The WAXD analysis was used to investigate the crystal structure of different copolyester fibers, and the WAXD patterns were shown in Figure 6, together with the deconvoluted peaks using PeakFit v4 curve-fitting software. The diffraction peaks of CDP fiber at 2θ of 18, 22.5, and 25.9°, which were also the characteristic diffraction peaks of triclinic PET, corresponding to (010), (1$\bar{1}$0), and (010) reflection planes, respectively, suggesting that SIP unit did not pack into the original polyester unit cell.[12,28] The diffraction peaks of PCDP, MCDP, and NCDP fibers were not found to obviously shift except for the diffraction intensities when compared with that of CDP fiber, suggesting that the crystal structure in each copolyester fiber was also triclinic system in the same manner as PET. Therefore, only the PET segments in each copolyester fiber were capable of crystallization, and PDO, MPD, and NPG units, as well as SIP unit, were excluded from the crystal regions.

For each copolyester fiber, the crystallinity derived from the areas of the crystal reflection peaks and the broad amorphous curve, the crystallite size determined using Scherrer's equation, and the interplanar distance calculated according to Bragg's law were listed in Table VI. It could be seen that both crystallinity and crystal size decreased in the order of CDP, PCDP, MCDP, and NCDP fibers. As mentioned earlier, these might result from the fact that the fourth unit destroyed the regularity of the macromolecular chain and the branched methyl groups further hindered the motion of the PET segment and disturbed the crystal growth during spinning and drawing. Although less prominent, the interplanar distance tended to increase very slightly in the order of CDP, PCDP, MCDP, and NCDP fibers, implying that introducing PDO, MPD, and NPG units into the macromolecular chain also led to the looser crystal structure.

Mechanical Properties of Copolyester Fibers

The mechanical properties of the copolyester fibers were shown in Table VII. In the case of almost identical fineness of 100 denier/36 filament, the copolyester fiber containing the fourth unit generally had lower tensile strength but higher elongation than CDP fiber, indicating that the flexible chain segments of the fourth units decreased the macromolecular chains rigidity. The tensile strength and the breaking elongation slightly decreased in the order of PCDP, MCDP, and NCDP fibers, implying that the branched methyl groups played a negative effect on the mechanical properties of the copolyester fibers. The breaking strength of PCDP, MCDP, or NCDP fiber was lower than that of CDP fiber but still above 2.2 cN/dtex, suggesting that these copolyester fibers could also be suitable for the consequent textile processing. Moreover, compared with CDP fiber, the copolyester fiber containing the fourth unit generally exhibited lower initial modulus, meaning that they would be softer than CDP fiber, which were consistent with actual hand feeling.

Dyeability of Copolyester Fibers

Our attempt in this study was optimal selection of the three kinds of diols as the fourth monomer for dyeability improvement of copolyester. The dyeability of copolyester fibers dyeing at boiling temperature under normal pressure was shown in Table VIII. Dyeing experiments in disperse dyebath might contribute to the understanding of the accessible region of dyestuff molecule in copolyester fiber. Since the accessible region of

Table VII. Mechanical Properties and Dyeability of Copolyester Fibers

Sample code	Breaking strength (cN/dtex)	Breaking elongation (%)	Initial modulus (cN/dtex)
CDP	2.95	20.5	90.3
PCDP	2.67	31.6	58.6
MCDP	2.54	28.9	60.5
NCDP	2.25	27.6	63.2

Table VIII. Dyeability of Copolyester Fibers

Sample code	Dye uptake (%)	
	Disperse Red HLE	Cationic Red X-GRL
CDP	85.2	48.6
PCDP	89.6	61.3
MCDP	94.2	91.9
NCDP	90.2	85.6

dyestuff molecule only was amorphous region assuming a two-phase model of crystalline regions and amorphous regions described for fiber structure, disperse dye uptake in fiber was correlated with the quantity and structure of the amorphous region.[29] Table VIII showed that the disperse dye uptake value of the copolyester fiber containing the fourth unit generally was higher than that of CDP fiber at the same dyeing conditions. As mentioned earlier, introducing the fourth unit into the macromolecular chain depressed the crystallization ability of copolyester, the copolyester fiber had larger amorphous region and lower crystallinity which benefited the diffusion of dyestuff molecule. However, NCDP fiber had the largest amorphous region and the lowest crystallinity among the copolyester fibers, but its disperse dye uptake value was lower than that of MCDP fiber. On one hand, the branched methyl groups increased free volume and led to looser structure of the amorphous region, thereby the accessible region of dyestuff molecule increased. On the other hand, the branched methyl groups had the steric hindrance effect which could blocked the movement of dyestuff molecule. For NCDP fiber, each NPG unit possessed the two branched methyl groups; therefore, the steric hindrance effect was considered as one of major reasons for its lower disperse dye uptake value when compared with MCDP fiber.

During dyeing of the copolyester fiber in cationic dyebath, the anionic group $-SO_3^-$ exchanged counterions Na^+ with dye cations, resulting in cationic dye bonded to anionic groups in the fiber.[30] Therefore, the SIP content in the copolyester was one of the major factors for cationic dye uptake in fibers. Because each copolyester possessed almost identical SIP unit content (see Table III), similar to disperse dye, cationic dye uptake at the same dyeing conditions also depended on the quantity and structure of the amorphous region in the fiber, which was also the accessible region of cationic dyestuff molecule diffusion. Table VI showed that CDP fiber dyeing at 100°C under normal pressure had the lowest cationic dye uptake value when compared with the other fibers, so in practical producing the dyeing conditions of high temperature and high pressure were required. The cationic dye uptake values of PCDP, MCDP, and NCDP fibers dyeing at 100°C under normal pressure generally increased when compared with CDP fiber, indicating that the fourth units generally improved the cationic dyeability of copolyester fibers. As expected, the trend of cationic dye uptake values changing of PCDP, MCDP, and NCDP was in agreement with that of disperse dye uptake values, and MCDP fiber had the highest cationic dye uptake value, which further confirmed that MCDP fiber possessed a more looser, more accessible structure for both disperse dye and cationic dye.

CONCLUSIONS

The sulfonated copolyesters were modified by PDO, MPD, and NPG, respectively. During synthesis of these copolyesters, esterification might be accelerated by PDO but delayed by MPD and NPG successively; polycondensation time was extended in the order of PCDP, MCDP, and NCDP, and stirring torque in late polycondensation period relatively linearly rose which was different from remarkable increasing in the case of CDP. The structures of copolyesters were confirmed by FTIR and NMR spectra, consistent with the expected structures. The copolyesters possessed nearly identical SIP contents and almost the same fourth unit contents. The IV values, DEG contents, CEG contents, and color of copolyesters were also discussed. Phase transition behavior measured by DSC revealed that incorporation of PDO, MPD, and NPG successively led to a more irregular chain structure and thereby inhibited chain packing for crystallization. The good spinnability of CDP, PCDP, and MCDP and the relatively poor spinnability of NCDP were observed by the spinning and drawing experiments. WAXD patterns of copolyester fibers confirmed that only PET segments could be embedded into the crystal lattice, and both crystallinity and crystal size decreased in the order of CDP, PCDP, MCDP, and NCDP. Although the mechanical properties of PCDP, MCDP, and NCDP declined to some extent, they were still suitable to meet the requirements of textile. The fiber dyeing experiments revealed that incorporation of PDO, MPD, and NPG could improve the dyeability of copolyester fibers, and MCDP fiber had the best dyeability at boiling temperature under normal pressure for both disperse dye and cationic dye among these copolyester fibers. This study provided a reference for optimal selection on these three kinds of diols for cationic dyeable copolyester.

REFERENCES

1. Datye, K. V. *J. Text. Assoc.* **1994**, *42*, 55.
2. Maycumber, S. *Daily News Record* **1999**, *29*, 10.
3. Silkstone, K. *Rev. Prog. Colorat.* **1982**, *12*, 22.
4. Teli, M. D.; Prasad, N. M.; Vyas, U. V. *J. Appl. Polym. Sci.* **1993**, *50*, 449.
5. Pal, S. K.; Gandhi, R. S.; Kothari, V. K. *J. Appl. Polym. Sci.* **1996**, *61*, 401.
6. Liu, Z.; Zhai, L. *Syn. Fib. Ind.* **1991**, *6*, 15.
7. Dave, J.; Kumar, R.; Srivastava, H. *J. Appl. Polym. Sci.* **1987**, *33*, 455.
8. Eisenberg, A.; Hird, B.; Moore, R. *Macromolecules* **1990**, *23*, 4098.
9. Guo, X.; Gu, L.; Feng, X. *J. Appl. Polym. Sci.* **2002**, *86*, 3660.
10. Hong, Z. *Appl. Polym. Sci.* **1987**, *34*, 1353.
11. Timm, D. A.; Hsieh, Y. L. *J. Polym. Sci.: Polym. Phys. Ed.* **1993**, *31*, 1873.
12. Chen, B.; Gu, L. *J. Appl. Polym. Sci.* **2010**, *117*, 2454.
13. Chen, B.; Zhong, L. *J. Appl. Polym. Sci.* **2010**, *116*, 2487.
14. Wei, G.; Wang, L.; Chen, G. *J. Appl. Polym. Sci.* **2006**, *100*, 1511.

15. Lewis, C. L.; Spruiell, J. E. *J. Appl. Polym. Sci.* **2006**, *100*, 2592.
16. Tsuyoshi, K.; Tsuyoshi, M.; Naoto, T. *Polymer* **1994**, *35*, 1274.
17. Soleimani-Gorgani, A.; Taylor, J. A. *Dyes Pigm.* **2008**, *76*, 610.
18. Wu, R. R.; Zhang, T. J. Synthesis and Modification of Spinnable Polymer; Petrochemical industry publishing house of China: Beijing, **2003**.
19. El-Toufaili, F. A.; Feix, G.; Reichert, K. H. *J. Polym. Sci. Part A: Polym. Chem.* **2006**, *44*, 1049.
20. Wang, L. *Syn. Fib.* **2002**, *3*, 35.
21. Macomber, R. S. A Complete Introduction to Modern NMR Spectroscopy, 1st ed.; Wiley-Interscience: New York, **1998**.
22. De Ilarduya, A. M.; Kint, D. P. R.; Munoz-Guerra, S. *Macromolecules* **2000**, *33*, 4596.
23. Berr, C. E. *J. Polym. Sci.* **1955**, *15*, 591.
24. Mondek, L.; Malek, J. *Makromol. Chem.* **1977**, *178*, 2211.
25. Kint, D. P. R.; Ilarduya, A. M. D. *J. Polym. Sci.: Part A: Polym. Chem.* **2000**, *38*, 1934.
26. James, D. E.; Packer, L. G. *Ind. Eng. Chem. Res.* **1995**, *34*, 4049.
27. Wang, C.; Li, J.; Han, Q.; Wang, H.; Ding, J. *Syn. Fib. Ind.* **2009**, *5*, 33.
28. Hsiao, K. J.; Jen, Z. F.; Lu, C. L. *J. Appl. Polym. Sci.* **2002**, *86*, 3601.
29. Radhakrishnad, J.; Kanitkar, U. P.; Gupta, V. B. *J. Soc. Dy. Col.* **1997**, *113*, 59.
30. Ostrowska, B.; Narebska, A. *J. Appl. Polym. Sci.* **1981**, *26*, 643.